Canadian Mineralogist
Vol. 31, pp. 321-329 (1993)

EDGE-SHARING $Mn^{2+}O_4$ TETRAHEDRA IN THE STRUCTURE OF AKATOREITE, $Mn_9^{2+}Al_2Si_8O_{24}(OH)_8$

PETER C. BURNS AND FRANK C. HAWTHORNE

Department of Geological Sciences, University of Manitoba, Winnipeg, Manitoba R3T 2N2

ABSTRACT

The crystal structure of akatoreite, $Mn_9^{2+}Al_2Si_8O_{24}(OH)_8$, *a* 8.337(2), *b* 10.367(2), *c* 7.629(1) Å, α 104.46(1), β 93.81(2), γ 104.18(1)°, *V* 613.2(2) Å^3, $P\bar{1}$, *Z*=1, has been solved by direct methods and refined to an *R* index of 2.9% for 2691 observed reflections measured with Mo*K*α radiation. There are five independent Mn positions. Four of these are octahedrally coordinated by O^{2-} and OH^- anions, and the mean bond-lengths at these sites show the Mn to be entirely in the divalent state. The fifth Mn position is tetrahedrally coordinated by four O^{2-} anions, and the mean bond-length shows the Mn to be in the divalent state. Adjacent (MnO_4) tetrahedra share an edge to form an [Mn_2O_6] dimer. There is one Al position, coordinated by six anions in an octahedral arrangement, and both site-scattering refinement and mean bond-length show no substitution of Fe^{3+} or Mn^{3+} for Al at this site. There are four distinct Si positions, all of which are tetrahedrally coordinated; one of the silicate tetrahedra is an acid silicate group: $SiO_3(OH)$. The four Si tetrahedra form a linear [$Si_4O_{12}(OH)$] cluster, and akatoreite is thus a sorosilicate. The ($Mn\phi_6$) and ($Al\phi_6$) octahedra (φ: unspecified anion) form edge-sharing strips of octahedra, three octahedra wide, that extend along the *a* direction. These strips are cross-linked into sheets by the [Mn_2O_6] tetrahedral dimers, which share edges with the peripheral octahedra of adjacent strips. The resultant sheets are linked into a complex heteropolyhedral framework by the sorosilicate fragments and by a hydrogen-bond network. Relationships to other sorosilicates are reviewed.

Keywords: akatoreite, crystal structure, silicate, sorosilicate, tetrahedrally coordinated divalent manganese.

SOMMAIRE

Nous avons affiné la structure cristalline de l'akatoréite, $Mn_92+Al_2Si_8O_{24}(OH)_8$, *a* 8.337(2), *b* 10.367(2), *c* 7.629(1) Å, α 104.46(1), β 93.81(2), γ 104.18(1)°, *V* 613.2(2) Å^3, $P\bar{1}$, *Z* = 1, par méthodes directes jusqu'à un résidu *R* de 2.9% en utilisant 2691 réflexions observées, mesurées avec rayonnement Mo*K*α. La structure contient cinq sites indépendants de Mn. Quatre d'entre eux sont en coordinence octaédrique avec des anions O^{2-} et OH^-; dans chaque cas, la longueur moyenne des liaisons montre que le Mn est entièrement bivalent. Le Mn de la cinquième position possède une coordinence tétraédrique avec quatre anions O^{2-}; la longueur moyenne des liaisons montre que le Mn est bivalent. Les tétraèdres (MnO_4) adjacents partagent une arête, pour former un dimère [Mn_2O_6]. Il y a une position occupée par l'Al, entourée de six anions formant un octaèdre. Un affinement des pouvoirs de dispersion à cette position, aussi bien que la longueur moyenne des liaisons, montrent qu'il n'y a aucun remplacement de l'Al par Fe^{3+} ou Mn^{3+}. La structure comporte quatre positions distinctes occupées par Si, toutes à coordinence tétraédrique. Dans un cas, il s'agit d'un groupe silicaté acide: $SiO_3(OH)$. Les quatre tétraèdres Si forment un alignement [$Si_4O_{12}(OH)$]; l'akatoréite serait donc un sorosilicate. Les octaèdres ($Mn\phi_6$) et ($Al\phi_6$) forment des rubans d'octaèdres à arêtes partagées, d'une largeur de trois octaèdres, orientés le long de *a*. Ces rubans sont liés transversalement en feuillets par les dimères de tétraèdres [Mn_2O_6], qui partagent une arête avec l'octaèdre périphérique des rubans adjacents. Les feuillets qui en résultent sont liés en une trame complexe hétéropolyédrique par les fragments sorosilicatés et un réseau de liaisons hydrogène. Nous examinons la relation de cette structure avec celle d'autres sorosilicates.

(Traduit par la Rédaction)

Mots-clés: akatoréite, structure cristalline, silicate, sorosilicate, manganèse bivalent à coordinence tétraédrique.

INTRODUCTION

Akatoreite is a hydrous manganese aluminosilicate first described by Read & Reay (1971). It occurs as vitreous, orange-brown, massive to radiating twinned columnar aggregates in a manganiferous metachert and carbonate lens on the southeastern margin of the Haast Schist Group, South Island, New Zealand. Akatoreite is associated with rhodochrosite, rhodonite, spessartine, quartz, hübnerite, alabandite, pyroxmangite, tinzenite, apatite, psilomelane, pyrolusite and todorokite.

Results of chemical analyses reported by Read & Reay (1971) indicate that akatoreite has the formula $(Mn_{8.61}Fe_{0.19}Mg_{0.08}Ca_{0.05})Al_{2.09}Si_{7.75}O_{23.17}(OH)_{8.83}$. This

structural study results in revision of the akatoreite formula, which may be given ideally as $Mn_9Al_2Si_8O_{24}(OH)_8$.

Experimental

The material used in this work is from the type locality, 3 km south of the mouth of Akatore Creek, eastern Otago, New Zealand. An optical examination of the akatoreite crystals indicated that it is usually twinned, as reported by Read & Reay (1971). Several crystals of akatoreite were crushed and examined optically; a small untwinned cleavage fragment was eventually selected for study. The crystal was mounted on a Nicolet *R*3*m* automated four-circle diffractometer, and twenty-four reflections were centered using graphite monochromated Mo*K*α X-radiation. The unit-cell dimensions (Table 1) were derived from the setting angles of the twenty-four automatically aligned reflections by least-squares techniques. Data were collected using the θ–2θ scan method with a scan range of 2.4°2θ. A variable scan-rate inversely proportional to the peak intensity was used, with maximum and minimum scan-rates of 29°2θ/min and 4°2θ/min, respectively. A total of 3850 reflections was measured over the range $3° \leq 2\theta \leq 60°$, with index ranges $-12 \leq h \leq 12$, $-15 \leq k \leq 15$, $0 \leq l \leq 11$. Two standard reflections were measured every fifty reflections; no significant changes in their net intensities occurred during data collection. An empirical absorption correction based on 252 psi-scans collected for seven reflections over the range 14 to 47° 2θ was applied, which reduced *R* (azimuthal) from 4.6% to 2.4%. The data were corrected for Lorentz, polarization and background effects; of the 3850 reflections measured, there were 2691 unique observed reflections [$|F_O| \geq 5\sigma(F_O)$].

Structure Solution and Refinement

Scattering curves for neutral atoms, together with anomalous dispersion corrections, were taken from Cromer & Mann (1968) and Cromer & Liberman (1970), respectively. *R* indices are of the form given in Table 1 and are expressed as percentages. The Siemens SHELXTL PLUS (PC version) system of programs was used throughout this work.

The possible space-groups of akatoreite are *P*1 and $P\bar{1}$. Reflection statistics indicated that $P\bar{1}$ was the most probable, and this space group was verified by the successful solution and refinement of the structure. The structure of akatoreite was solved by direct methods. The locations of five Mn, one Al, three Si and ten O positions were obtained from the solution with the highest combined figure of merit. Refinement of the positional parameters of this model converged to an *R* index of 28%. A three-dimensional difference-Fourier map calculated at this stage of the refinement revealed the location of an additional Si and six additional O

TABLE 1. MISCELLANEOUS INFORMATION FOR AKATOREITE

a (Å)	8.337(2)	Space group	$P\bar{1}$
b (Å)	10.367(2)	Crystal Size (mm)	0.06 x 0.12
c (Å)	7.629(1)		x 0.16
α (°)	104.46(1)	Total ref.	3850
β (°)	93.81(2)	$\|F_O\| \geq 5\sigma(F_O)$	2691
γ (°)	104.18(1)	Final *R*	2.9
V (Å^3)	613.2(2)	Final *wR*	3.2
F(000)	627		
Unit-cell contents		$[Mn_9Al_2Si_8O_{24}(OH)_8]$	

$R = \Sigma(||F_O| - |F_C||)/\Sigma|F_O|$

$wR = [\Sigma w(|F_O| - |F_C|)^2/\Sigma F_O^2]^{1/2}$, w=1

TABLE 2. ATOMIC PARAMETERS FOR AKATOREITE

	x	*y*	*z*	U_{equiv}*
Mn(1)	0	1/2	1/2	87(2)
Mn(2)	0.60854(7)	0.42848(6)	0.36083(8)	85(2)
Mn(3)	0.83621(7)	0.29882(6)	0.08032(8)	79(2)
Mn(4)	0.56978(7)	0.77338(6)	0.05242(8)	77(2)
Mn(5)	0.83542(8)	0.94289(6)	0.37937(8)	102(2)
Al(1)	0.2210(1)	0.3686(1)	0.2332(1)	54(3)
Si(1)	0.1155(1)	0.3580(1)	-0.1861(1)	54(3)
Si(2)	-0.4317(1)	0.1019(1)	-0.7056(1)	57(3)
Si(3)	-0.2559(1)	0.2987(1)	-0.3211(1)	56(3)
Si(4)	0.1910(1)	0.0480(1)	0.1988(1)	60(3)
O(1)	0.1671(3)	0.4991(3)	-0.2526(4)	79(8)
O(2)	0.0953(3)	0.3845(3)	0.0294(3)	81(8)
O(3)	-0.2330(3)	0.4429(3)	-0.3805(4)	75(8)
O(4)	-0.3370(3)	0.3047(3)	-0.1358(4)	92(8)
O(5)	0.2433(4)	0.2643(3)	-0.2440(4)	93(8)
O(6)	-0.3956(3)	0.2212(3)	-0.8120(4)	94(8)
O(7)	-0.3449(4)	-0.0198(3)	-0.7737(4)	108(8)
O(8)	-0.3682(4)	0.1741(3)	-0.6894(4)	118(8)
O(9)	-0.0716(3)	0.2701(3)	-0.3002(4)	92(8)
O(10)	0.0750(3)	0.0573(3)	0.3611(4)	92(8)
O(11)	0.3678(3)	0.0348(3)	0.2767(4)	115(9)
O(12)	0.2138(3)	0.1800(3)	0.1161(4)	78(8)
OH(13)	0.0168(3)	0.3125(3)	0.3242(4)	73(8)
OH(14)	0.3626(3)	0.3680(3)	0.4465(4)	80(8)
OH(15)	0.1094(4)	-0.0957(3)	0.0348(4)	110(8)
OH(16)	0.4247(3)	0.4265(3)	0.1448(4)	86(8)
H(1)	0.035(7)	0.235(4)	0.366(7)	150**
H(2)	0.330(7)	0.291(4)	0.501(7)	150
H(3)	-0.012(1)	-0.120(6)	0.004(7)	150
H(4)	0.424(7)	0.513(3)	0.118(7)	150

* $U_{equiv} = U_{equiv} \times 10^4$

** fixed during refinement

TABLE 3. ANISOTROPIC DISPLACEMENT PARAMETERS (x10^4) FOR AKATOREITE

	U_{11}	U_{22}	U_{33}	U_{23}	U_{13}	U_{12}
Mn(1)	90(3)	97(4)	74(3)	14(3)	30(3)	28(3)
Mn(2)	80(2)	97(3)	71(2)	12(2)	13(2)	22(2)
Mn(3)	76(2)	92(3)	73(2)	25(2)	17(2)	27(2)
Mn(4)	83(2)	78(3)	71(2)	20(2)	20(2)	20(2)
Mn(5)	103(3)	94(3)	100(3)	39(2)	-8(2)	7(2)
Al(1)	60(4)	57(5)	50(4)	18(4)	19(4)	21(4)
Si(1)	66(4)	59(4)	49(4)	29(3)	21(3)	20(3)
Si(2)	70(4)	48(4)	58(4)	26(3)	14(3)	12(3)
Si(3)	69(4)	63(4)	43(4)	27(3)	11(3)	17(3)
Si(4)	67(4)	57(4)	57(4)	17(3)	11(3)	13(3)
O(1)	98(12)	76(12)	80(12)	44(10)	40(9)	21(10)
O(2)	96(12)	93(12)	61(12)	36(10)	22(9)	19(10)
O(3)	110(12)	57(11)	63(11)	20(9)	24(9)	26(9)
O(4)	93(12)	124(13)	63(12)	32(10)	29(10)	25(10)
O(5)	110(12)	105(12)	85(12)	30(10)	32(10)	60(10)
O(6)	112(12)	90(12)	87(12)	46(10)	33(10)	15(10)
O(7)	134(13)	95(12)	104(13)	23(10)	26(10)	52(10)
O(8)	166(13)	105(13)	55(12)	18(10)	-6(10)	-2(10)
O(9)	87(12)	110(12)	90(12)	36(10)	5(10)	39(10)
O(10)	91(12)	119(13)	75(12)	45(10)	22(10)	22(10)
O(11)	77(12)	101(13)	181(14)	93(11)	0(10)	0(10)
O(12)	113(12)	56(12)	65(12)	13(9)	3(9)	28(10)
OH(13)	87(12)	77(12)	70(12)	40(10)	40(9)	25(10)
OH(14)	94(12)	74(12)	88(12)	37(10)	22(9)	33(9)
OH(15)	128(13)	87(12)	94(12)	-1(10)	-12(10)	24(10)
OH(16)	98(12)	91(12)	82(12)	37(10)	30(10)	31(10)

TABLE 4. SELECTED INTERATOMIC DISTANCES (Å), ANGLES (°) AND POLYHEDRAL EDGE-LENGTHS (Å) IN AKATOREITE

Mn(1)-O(1)a x2	2.274(3)	Al(1)-O(2)	1.882(3)
Mn(1)-O(3)b x2	2.213(3)	Al(1)-O(3)i	1.971(3)
Mn(1)-OH(13) x2	2.110(3)	Al(1)-O(12)	1.920(3)
<Mn(1)-O>	2.199	Al(1)-OH(13)	1.895(3)
		Al(1)-OH(14)	1.948(3)
Mn(2)-O(1)c	2.138(3)	Al(1)-OH(16)	1.885(3)
Mn(2)-O(3)d	2.252(3)	<Al-O>	1.917
Mn(2)-O(6)e	2.214(3)		
Mn(2)-OH(14)f	2.197(3)	Si(1)-O(1)	1.635(3)
Mn(2)-OH(14)	2.186(3)	Si(1)-O(2)	1.625(3)
Mn(2)-OH(16)	2.168(3)	Si(1)-O(5)	1.621(3)
<Mn(2)-O>	2.192	Si(1)-O(9)	1.658(3)
		<Si(1)-O>	1.635
Mn(3)-O(1)c	2.186(3)		
Mn(3)-O(2)g	2.225(3)	Si(2)-O(6)	1.621(3)
Mn(3)-O(4)g	2.141(3)	Si(2)-O(7)	1.599(3)
Mn(3)-O(6)e	2.200(3)	Si(2)-O(8)	1.623(3)
Mn(3)-OH(13)q	2.267(3)	Si(2)-O(11)m	1.628(3)
Mn(3)-OH(15)h	2.238(3)	<Si(2)-O>	1.618
<Mn(3)-O>	2.209		
		Si(3)-O(3)	1.639(3)
Mn(4)-O(4)i	2.116(3)	Si(3)-O(4)	1.601(3)
Mn(4)-O(5)j	2.236(3)	Si(3)-O(8)	1.617(3)
Mn(4)-O(6)k	2.284(3)	Si(3)-O(9)	1.640(3)
Mn(4)-O(7)l	2.138(3)	<Si(3)-O>	1.624
Mn(4)-O(12)h	2.310(3)		
Mn(4)-OH(16)i	2.249(3)	Si(4)-O(10)	1.619(3)
<Mn(4)-O>	2.222	Si(4)-O(11)	1.603(3)
		Si(4)-O(12)	1.621(3)
Mn(5)-O(5)j	2.055(3)	Si(4)-OH(15)	1.645(3)
Mn(5)-O(7)l	2.012(3)	<Si(4)-O>	1.622
Mn(5)-O(10)m	2.091(3)		
Mn(5)-O(10)f	2.070(3)		
<Mn(5)-O>	2.057		

Hydrogen bonding

OH(13)-H(1)	0.97(5)	H(1)...O(10)	1.94(5)
OH(14)-H(2)	0.98(5)	H(2)...O(5)b	2.17(5)
OH(15)-H(3)	0.98(1)	H(3)...O(12)o	1.75(2)
OH(16)-H(4)	0.97(4)	H(4)...O(4)i	2.16(4)
OH(13)-O(10)	2.881(5)	OH(13)-H(1)-O(10)	160(5)
OH(14)-O(5)b	2.962(4)	OH(14)-H(2)-O(5)b	137(4)
OH(15)-O(12)o	2.698(4)	OH(15)-H(3)-O(12)o	163(4)
OH(16)-O(4)i	3.064(5)	OH(16)-H(4)-O(4)i	154(5)

Mn(4) octahedron

O(4)i-O(5)j	3.439(4)	O(4)i-Mn(4)-O(5)j	104.4(1)
O(4)i-O(6)k	2.849(4)	O(4)i-Mn(4)-O(6)k	80.6(1)
O(4)i-O(7)l	3.336(4)	O(4)i-Mn(4)-O(7)l	103.3(1)
O(4)i-OH(16)j	3.251(4)	O(4)i-Mn(4)-OH(16)j	96.2(1)
O(5)j-O(7)l	2.893(5)	O(5)j-Mn(4)-O(7)l	82.8(1)
O(5)j-O(12)h	3.092(4)	O(5)j-Mn(4)-O(12)h	85.7(1)
O(5)j-OH(16)j	3.095(4)	O(5)j-Mn(4)-OH(16)j	87.3(1)
O(6)k-O(7)l	3.552(4)	O(6)k-Mn(4)-O(7)l	106.8(1)
O(6)k-O(12)h	3.170(4)	O(6)k-Mn(4)-O(12)h	87.3(1)
O(6)k-OH(16)j	2.955(5)	O(6)k-Mn(4)-OH(16)j	81.4(1)
O(7)l-O(12)h	3.143(4)	O(7)l-Mn(4)-O(12)h	89.9(1)
O(12)h-OH(16)j	2.672(4)	O(12)h-Mn(4)-OH(16)j	71.7(1)
<O-O>	3.121	<O-Mn(4)-O>	89.8

Mn(5) tetrahedron

O(5)j-O(7)l	2.893(5)	O(5)j-Mn(5)-O(7)l	90.7(1)
O(5)j-O(10)m	3.580(4)	O(5)j-Mn(5)-O(10)m	119.4(1)
O(5)j-O(10)f	3.223(3)	O(5)j-Mn(5)-O(10)f	102.8(1)
O(7)l-O(10)m	3.419(4)	O(7)l-Mn(5)-O(10)m	112.8(1)
O(7)l-O(10)f	3.901(5)	O(7)l-Mn(5)-O(10)f	145.7(1)
O(10)m-O(10)f	2.889(6)	O(10)m-Mn(5)-O(10)f	87.9(1)
<O-O>	3.317	<O-Mn(5)-O>	109.9

Al(1) octahedron

O(2)-OH(16)	2.721(4)	O(2)-Al(1)-OH(16)	92.5(1)
O(2)-O(3)i	2.808(3)	O(2)-Al(1)-O(3)i	93.6(1)
O(2)-O(12)	2.784(5)	O(2)-Al(1)-O(12)	92.6(1)
O(2)-OH(13)	2.615(4)	O(2)-Al(1)-OH(13)	87.6(1)
OH(14)-OH(16)	2.576(4)	OH(14)-Al(1)-OH(16)	84.4(1)
OH(14)-O(3)i	2.593(5)	OH(14)-Al(1)-O(3)i	82.8(1)
OH(14)-O(12)	2.763(3)	OH(14)-Al(1)-O(12)	91.2(1)
OH(14)-OH(13)	2.842(4)	OH(14)-Al(1)-OH(13)	95.4(1)
OH(16)-O(3)i	2.801(4)	OH(16)-Al(1)-O(3)i	93.2(1)
OH(16)-O(12)	2.672(4)	OH(16)-Al(1)-O(12)	89.2(1)
O(3)i-OH(13)	2.641(4)	O(3)i-Al(1)-OH(13)	86.2(1)
O(12)-OH(13)	2.732(4)	O(12)-Al(1)-OH(13)	91.5(1)
<O-O>	2.709	<O-Al(1)-O>	90.0

Mn(1) octahedron

O(1)a-O(3)b x2	3.279(4)	O(1)a-Mn(1)-O(3)b x2	93.9(1)
O(1)a-O(3)i x2	3.063(4)	O(1)a-Mn(1)-O(3)i x2	86.1(1)
O(1)a-OH(13) x2	3.301(3)	O(1)a-Mn(1)-OH(13) x2	97.6(1)
O(1)a-OH(13)p x2	2.891(5)	O(1)a-Mn(1)-OH(13)p x2	82.4(1)
O(3)b-OH(13) x2	3.424(4)	O(3)b-Mn(1)-OH(13) x2	75.3(1)
O(3)b-OH(13)p x2	2.641(4)	O(3)b-Mn(1)-OH(13)p x2	104.7(1)
<O-O>	3.100	<O-Mn(1)-O>	90.0

Mn(2) octahedron

OH(14)-OH(16)	2.576(4)	OH(14)-Mn(2)-OH(16)	72.6(1)
OH(14)-O(3)d	3.366(4)	OH(14)-Mn(2)-O(3)d	98.6(1)
OH(14)-O(6)e	3.286(4)	OH(14)-Mn(2)-O(6)e	96.7(1)
OH(14)-OH(14)f	2.995(5)	OH(14)-Mn(2)-OH(14)f	86.2(1)
OH(16)-O(1)c	3.298(4)	OH(16)-Mn(2)-O(1)c	100.0(1)
OH(16)-O(6)e	2.955(5)	OH(16)-Mn(2)-O(6)e	84.8(1)
OH(16)-OH(14)f	3.392(3)	OH(16)-Mn(2)-OH(14)f	102.0(1)
O(1)c-O(3)d	3.063(4)	O(1)c-Mn(2)-O(3)d	88.5(1)
O(1)c-O(6)e	2.956(4)	O(1)c-Mn(2)-O(6)e	85.6(1)
O(1)c-OH(14)f	3.130(4)	O(1)c-Mn(2)-OH(14)f	92.4(1)
O(3)d-O(6)e	3.472(3)	O(3)d-Mn(2)-O(6)e	102.1(1)
O(3)d-OH(14)f	2.593(5)	O(3)d-Mn(2)-OH(14)f	71.3(1)
<O-O>	3.090	<O-Mn(2)-O>	90.1

Mn(3) octahedron

O(1)c-OH(13)g	2.891(5)	O(1)c-Mn(3)-OH(13)g	80.9(1)
O(1)c-O(2)g	3.147(4)	O(1)c-Mn(3)-O(2)g	91.1(1)
O(1)c-O(4)g	3.154(3)	O(1)c-Mn(3)-O(4)g	93.6(1)
O(1)c-O(6)e	2.956(4)	O(1)c-Mn(3)-O(6)e	84.8(1)
O(2)g-OH(15)h	2.962(4)	O(2)g-Mn(3)-OH(15)h	83.1(1)
O(2)g-O(4)g	3.561(4)	O(2)a-Mn(3)-O(4)q	109.3(1)
OH(13)g-O(2)g	2.615(4)	OH(13)g-Mn(3)-O(2)g	71.2(1)
OH(13)g-O(6)e	3.352(4)	OH(13)g-Mn(3)-O(6)e	97.3(1)
OH(13)g-OH(15)h	3.007(3)	OH(13)g-Mn(3)-OH(15)h	83.7(1)
O(4)g-O(6)e	2.849(4)	O(4)g-Mn(3)-O(6)e	82.0(1)
O(4)g-OH(15)h	3.398(5)	O(4)g-Mn(3)-OH(15)h	101.7(1)
O(6)e-OH(15)h	3.352(4)	O(6)e-Mn(3)-OH(15)h	98.1(1)
<O-O>	3.104	<O-Mn(3)-O>	89.7

Si(1) tetrahedron

O(1)-O(2)	2.737(4)	O(1)-Si(1)-O(2)	114.2(1)
O(1)-O(5)	2.676(5)	O(1)-Si(1)-O(5)	110.6(2)
O(1)-O(9)	2.624(4)	O(1)-Si(1)-O(9)	105.7(2)
O(2)-O(5)	2.687(4)	O(2)-Si(1)-O(5)	111.8(2)
O(2)-O(9)	2.627(4)	O(2)-Si(1)-O(9)	106.3(1)
O(5)-O(9)	2.649(4)	O(5)-Si(1)-O(9)	107.8(1)
<O-O>	2.667	<O-Si(1)-O>	109.4

Si(2) tetrahedron

O(6)-O(7)	2.715(5)	O(6)-Si(2)-O(7)	114.9(2)
O(6)-O(8)	2.632(4)	O(6)-Si(2)-O(8)	108.4(1)
O(6)-O(11)m	2.654(4)	O(6)-Si(2)-O(11)m	109.5(2)
O(7)-O(8)	2.618(4)	O(7)-Si(2)-O(8)	108.7(2)
O(7)-O(11)m	2.623(4)	O(7)-Si(2)-O(11)m	108.8(2)
O(8)-O(11)m	2.597(4)	O(8)-Si(2)-O(11)m	106.1(2)
<O-O>	2.640	<O-Si(2)-O>	109.4

Si(3) tetrahedron

O(3)-O(4)	2.689(4)	O(3)-Si(3)-O(4)	112.2(2)
O(3)-O(8)	2.628(4)	O(3)-Si(3)-O(8)	107.7(2)
O(3)-O(9)	2.649(5)	O(3)-Si(3)-O(9)	107.8(2)
O(4)-O(8)	2.662(4)	O(4)-Si(3)-O(8)	111.7(1)
O(4)-O(9)	2.671(4)	O(4)-Si(3)-O(9)	111.0(2)
O(8)-O(9)	2.606(4)	O(8)-Si(3)-O(9)	106.3(2)
<O-O>	2.651	<O-Si(3)-O>	109.4

Si(4) tetrahedron

O(10)-O(12)	2.684(4)	O(10)-Si(4)-O(12)	111.9(2)
O(10)-OH(15)	2.672(4)	O(10)-Si(4)-OH(15)	109.9(1)
O(10)-O(11)	2.616(4)	O(10)-Si(4)-O(11)	108.6(2)
O(12)-OH(15)	2.671(4)	O(12)-Si(4)-OH(15)	109.7(2)
O(12)-O(11)	2.660(5)	O(12)-Si(4)-O(11)	111.2(2)
OH(15)-O(11)	2.584(4)	OH(15)-Si(4)-O(11)	105.4(2)
<O-O>	2.648	<O-Si(4)-O>	109.4

a = x, y, z-1; b = x, y, z+1; c = 1-x, 1-y, -z; d = x+1, y, z+1; e = x+1, y, z-1; f = 1-x, 1-y, 1-z; g = x+1, y, z; h = 1-x, -y, -z; i = -x, 1-y, -z; j = 1-x, 1-y, -z; k = -x, 1-y, -z-1; l = x-1, y-1, z-1; m = x+1, y+1, z; n = 1-x, y, z-1; o = 2-x, -y, -z; p = -x, 1-y, 1-z

positions. Refinement of all parameters, including an isotropic displacement model, converged to an R index of 3.7%. Conversion to an anisotropic displacement model, together with the refinement of all parameters, led to convergence to an R index of 3.0% and a wR index of 3.2%. A model including a refinable structure-factor weighting scheme and an isotropic extinction correction was tried but did not lead to any improvement in the

TABLE 5. BOND-VALENCE* TABLE FOR AKATOREITE

	Mn(1)	Mn(2)	Mn(3)	Mn(4)	Mn(5)	Al(1)	Si(1)	Si(2)	Si(3)	Si(4)	H(1)	H(2)	H(3)	H(4)	Σ
O(1)	0.268 ×2↓	0.379	0.335				0.986								1.968
O(2)			0.303			0.535	1.014								1.852
O(3)	0.312 ×2↓	0.283				0.423			0.975						1.993
O(4)			0.376	0.402					1.084					0.15	2.012
O(5)				0.292	0.473		1.059					0.15			1.977
O(6)		0.312	0.323	0.262				1.025							1.922
O(7)				0.379	0.533			1.090							2.002
O(8)								1.020	1.037						2.057
O(9)							0.925		0.973						1.898
O(10)					0.454 0.429					1.031	0.20				2.114
O(11)								1.006		1.078					2.084
O(12)				0.246		0.484				1.025			0.25		2.005
OH(13)	0.408 ×2↓		0.273			0.517					0.80				1.998
OH(14)		0.335 0.326				0.449						0.85			1.960
OH(15)			0.293							0.959			0.75		2.002
OH(16)		0.351		0.286		0.530								0.85	2.017
Σ	1.976	1.986	1.903	1.870	1.889	2.938	3.984	4.141	4.071	4.093	1.0	1.0	1.0	1.0	

* bond-valence parameters from Brown (1981)

refinement. A three-dimensional difference-Fourier map calculated during the final stages of refinement revealed the locations of the four hydrogen positions. Subsequent cycles of refinement showed the hydrogen positions to be unlikely, as indicated by anomalously short O–H bond distances, a common feature of refinement of hydrogen positions using X-ray data. The soft constraint that each O–H bond distance should be ~0.98 Å was imposed by adding the constraints as additional weighted observations in the least-squares matrix. Note that only the O–H distances were constrained, and that each hydrogen position was free to refine around the associated oxygen. Refinement of all structural parameters, including the hydrogen positions, converged to an *R* index of 2.9% and a *wR* index of 3.2%. Final positional parameters and equivalent isotropic displacement parameters are given in Table 2, anisotropic displacement parameters, in Table 3, selected bond-distances, angles and polyhedral edge-lengths, in Table 4, and a bond-valence analysis, in Table 5; observed and calculated structure-factors may be obtained from the Depository of Unpublished Data, CISTI, National Research Council of Canada, Ottawa, Ontario K1A 0S2.

Discussion

Cation coordination

There are five unique Mn positions in the akatoreite structure. Mn(1) to Mn(4) are each coordinated by six anions in an octahedral arrangement, and the mean observed bond-lengths are all ~2.20 Å. This value is close to the sum of the empirical radii of Shannon (1976) for $^{[6]}Mn^{2+}$ and $^{[3]}O^{2-}$ of 2.19 Å, indicating that all of the octahedrally coordinated Mn is in the divalent state. Mn(1) lies on a center of symmetry; hence the two coordinating hydroxyl anionic groups are in a *trans* arrangement. Mn(2) is coordinated by three oxygen atoms and three hydroxyl anionic groups, and the latter are all in a *cis* arrangement (Table 4). For Mn(3), the two coordinating hydroxyl anionic groups are in a *cis* arrangement, and Mn(4) has only one coordinating hydroxyl anionic group.

Mn(5) is coordinated by four oxygen atoms in a tetrahedral arrangement. The <Mn–O> distance is 2.057 Å, close to the sum of the empirical radii for $^{[4]}Mn^{2+}$ and $^{[3]}O^{2-}$ of 2.02 Å, indicating that the Mn at this site is divalent. The Mn(5) tetrahedron is extremely distorted (Table 4), the O–Mn–O angles varying between 88° and 145°; this extreme distortion is the result of the unusual polyhedral linkage associated with the MnO_4 tetrahedra, and will be discussed in more detail later.

There is one unique Al position, coordinated by three oxygen atoms and three hydroxyl anionic groups in an octahedral arrangement, the hydroxyl anionic groups being in both *cis* and *trans* arrangements. The scattering and equivalent displacement factor both indicate that there is no substitution of Mn^{3+} or Fe^{3+} for Al at this site.

There are four Si positions, all tetrahedrally coordinated, and there is polymerization of the silicate tetrahe-

dra. The Si(2) and Si(3) tetrahedra have two bridging and two nonbridging bonds, whereas the Si(1) and Si(4) tetrahedra each have one bridging and three nonbridging bonds. Furthermore, the Si(4) tetrahedron is actually an acid silicate group, as one of the anions is a hydroxyl group.

Structural description

Akatoreite is truly one of Nature's masterpieces of complexity. Figure 1 shows a polyhedral view of the structure along the *a* axis. From this view, it is apparent that the structure consists of sheets of octahedra and tetrahedra parallel to (101). However, the sheet of tetrahedra only consists of silicate groups (Fig. 1), and hence the MnO_4 tetrahedra must occur in the (dominantly) octahedral sheet.

A view of the sheet of octahedra (Fig. 2) shows its extremely unusual nature. The Mn(1–4) octahedra and the Al octahedron share edges to form continuous strips, three octahedra wide, that extend along the *a* direction. These strips are cross-linked by $[Mn_2^{2+}O_6]$ edge-sharing dimers of tetrahedra (Fig. 2) that share edges with the Mn(4) octahedra of adjacent sheets. Not only is this linkage unusual from a structural viewpoint, it is also associated with some very unusual stereochemical features. Firstly, the long axis of the dimer of tetrahedra $[Mn_2O_6]$ that links adjacent strips of octahedra is inclined at approximately 45° to the *c* axis, and this considerably distorts the Mn(4) octahedron, with which it shares edges, by requiring that the O(5)–O(7) edge be strongly inclined rather than parallel to the *a* axis. In a graphically identical sheet built from holosymmetrical polyhedra, the long axis of each tetrahedral dimer would be parallel to the *c* axis. Hence the relative dispositions of adjacent strips of octahedra do not constitute an intrinsic property of the polyhedral linkage within this sheet, but must be dictated by the details of the silicate sheet.

The $[Mn_9Al_2\phi_{32}]$ sheet and sandwiching silicate sheets are shown in Figure 3. The silicate tetrahedra polymerize to form an $[Si_4\phi_{13}, \phi: O^{2-}, OH^-]$ sorosilicate fragment. These sorosilicate fragments match up with the large interstices between the strips of edge-sharing octahedra (Fig. 2), linking to both the octahedra of adjacent strips and to the shared edge of the $[Mn_2O_6]$ dimer of tetrahedra. It is in this linkage that we find the reason for the observed relative disposition of the strips

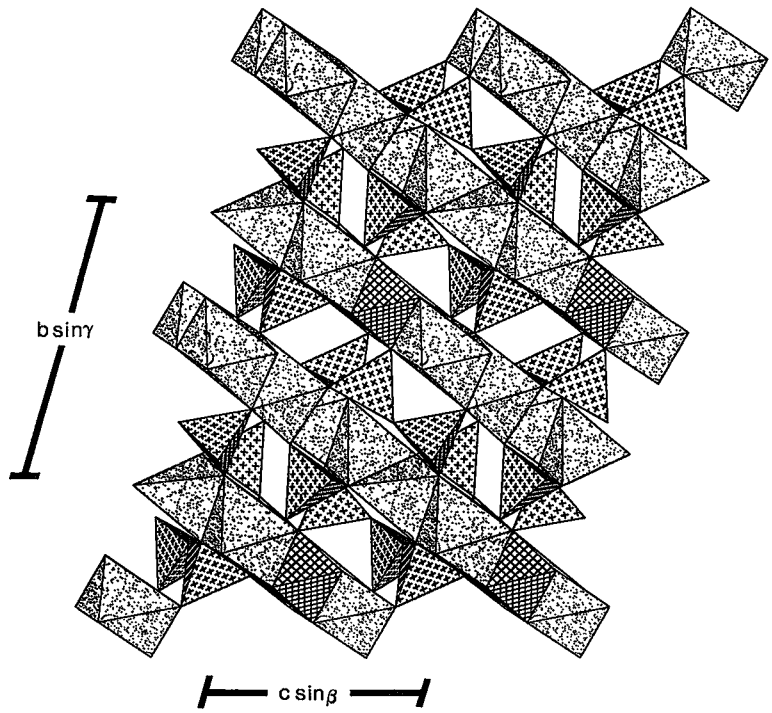

FIG. 1. Polyhedral representation of the structure of akatoreite projected along the *a* axis. The polyhedral shadings are as follows: Si: crosses, Al: cross-hatched, Mn: random dots. Note the compositional layering of the structure, with alternating layers of (SiO_4) tetrahedra and ($Mn\phi_6$), (MnO_4) tetrahedra and ($Al\phi_6$) octahedra.

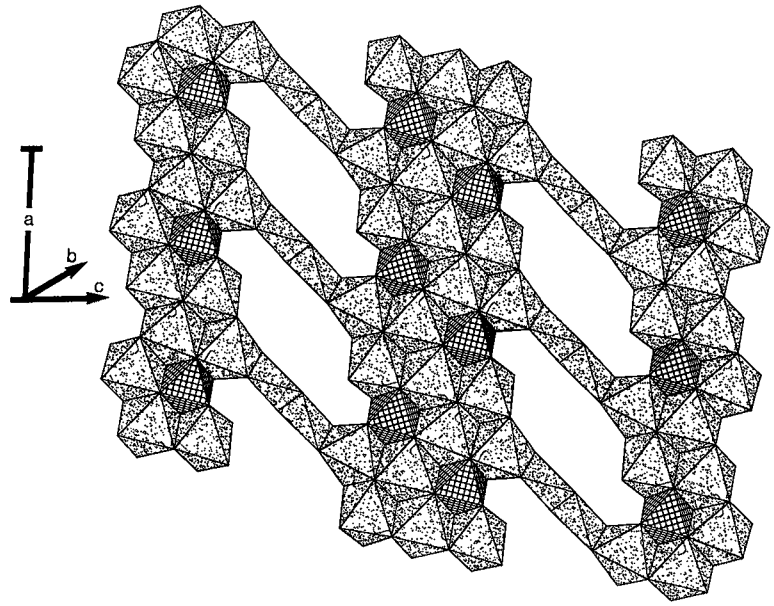

FIG. 2. Polyhedral representations of the structure of akatoreite: the $[Mn_9Al_2\phi_{22}]$ sheet projected on to (021); shading as in Figure 1. Strips of edge-sharing ($Mn\phi_6$) and ($Al\phi_6$) octahedra are centered along the *a* axis and are cross-linked by edge-sharing $[Mn_2O_6]$ dimers of tetrahedra.

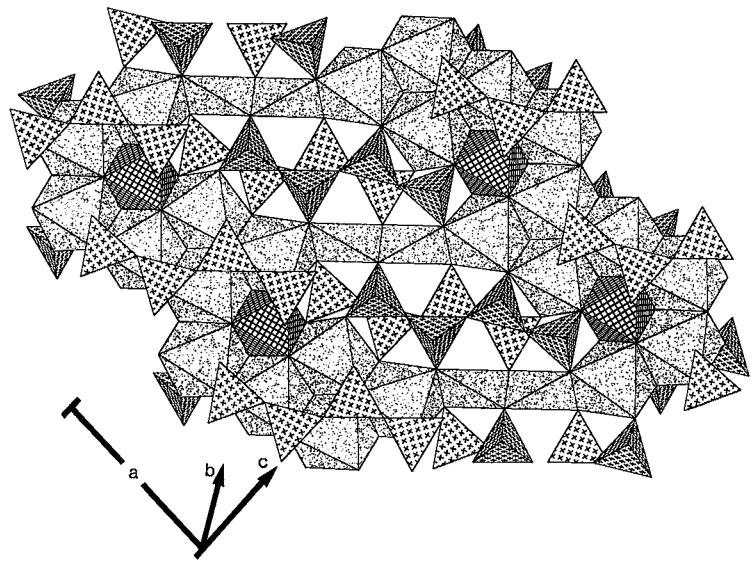

FIG. 3. Polyhedral representation of the structure of akatoreite projected onto (021); shadings as in Figure 1. The $[Mn_9Al_2\phi_{32}]$ sheet is shown with the sandwiching layers of silicate tetrahedra; note the $[Si_4\phi_{13}]$ sorosilicate fragments.

of octahedra and the dimers of tetrahedra. A SiO_4 tetrahedron links to both an O(10) of the shared edge of the $[Mn_2O_6]$ tetrahedral dimer and an anion of an $(Mn\phi_6)$ octahedron of the strip of octahedra. This linkage can only occur where adjacent strips are in their observed configuration; holosymmetrical polyhedra would lead to a corresponding distance too large to be the edge of a silicate tetrahedron.

The large interstices in the $[Mn_9Al_2\phi_{32}]$ sheet are sandwiched between $[Si_4\phi_{13}]$ sorosilicate fragments, and these back-to-back chain fragments resemble the relationship between adjacent silicate chains in the pyroxene structure. Sorosilicate fragments also link to the $[Mn_9Al_2\phi_{32}]$ sheet *via* one bond per tetrahedron, and this bond cross-links adjacent $[Mn_9Al_2\phi_{32}]$ sheets into a complex heteropolyhedral framework.

Hydrogen bonding

There are four unique hydrogen positions in akatoreite; details of their local stereochemistry are given in Table 4 and Figures 4 and 5. Three of the four hydrogen bonds link across adjacent $[Mn_9Al_2\phi_{32}]$ sheets (Fig. 4); the acceptor anions are always [3]-coordinated and never involve anions that bridge silicate tetrahedra. The H(3) atom hydrogen bonds to an adjacent O(12) anion within the same $[Mn_9Al_2\phi_{32}]$ sheet (Fig. 5); note that H(3) is bonded to an oxygen of a silicate tetrahedron, forming an acid (SiO_3OH) group. The D(donor)–H(hydrogen) distances are all approximately 0.98 Å, as forced by the soft-constraint method of the hydrogen-position refinement procedure. However, this procedure does not explicitly constrain the H(hydrogen)–A(acceptor) dis-

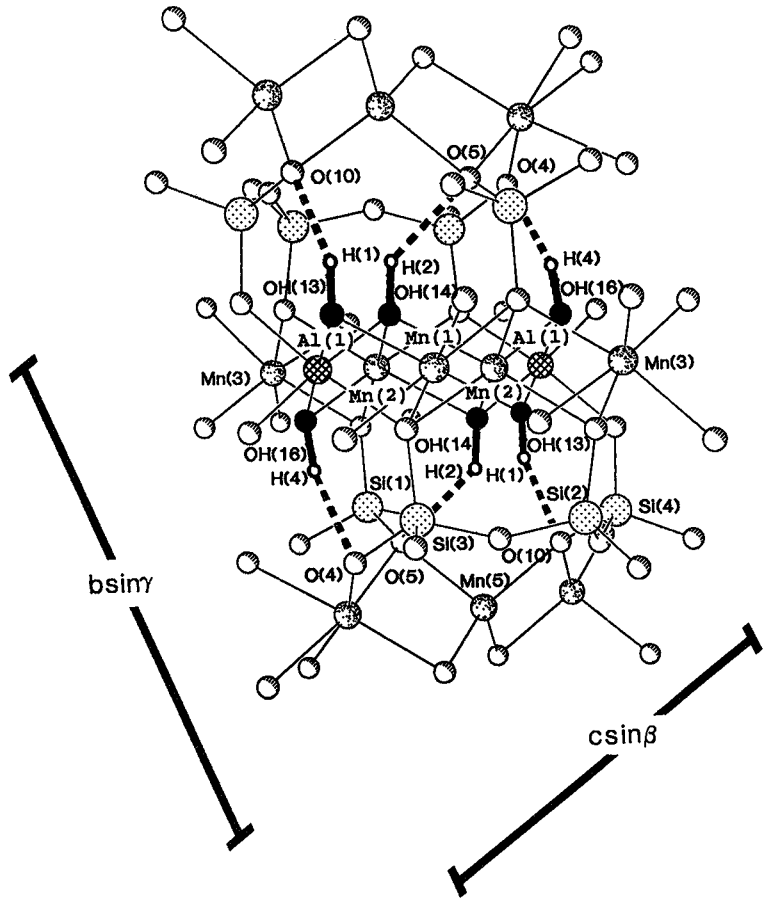

FIG. 4. The hydrogen-bonding arrangements involving the H(1), H(2) and H(4) atoms in akatoreite; cation shadings correspond to the polyhedral shadings of Figure 1, oxygen atoms are part-shaded spheres, hydrogen atoms are black spheres, donor–hydrogen and hydrogen–acceptor bonds are shown by heavy full and broken lines, respectively.

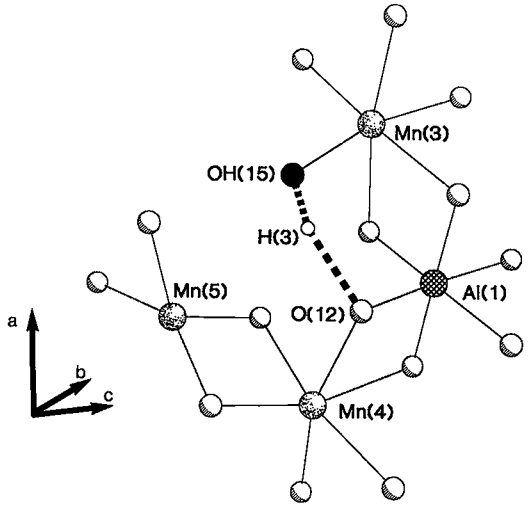

FIG. 5. The hydrogen-bonding arrangement involving the H(3) atom in akatoreite; legend as in Figure 4.

tances. These values lie between 1.75 and 2.17 Å, in the range for the occurrence of significant hydrogen bonding. In addition, the angles also are quite typical; three of the D–H–A angles are close to 160°, about the average for such angles in inorganic structures, and the fourth angle is 137°, within the range typical for minerals and inorganic structures.

The calculated H–A bond valences (Table 5) are in line with the other bond valences in the structure. The H(3)–O(12) distance of 1.75 Å (Table 4) is significantly shorter than the other H–A distances, and the variation in bond valence assigned to the O–H and H–A bonds leads to bond-valence sums around the donor and acceptor anions close to the ideal value of 2.0 v.u. (valence units).

Revision of the akatoreite formula

Read & Reay (1971) defined akatoreite as a hydrous manganese aluminosilicate with the formula $(Mn_{8.61}Fe_{0.19}Mg_{0.08}Ca_{0.05})Al_{2.09}Si_{7.75}O_{23.17}(OH)_{8.83}$. This formula was based upon results of electron-microprobe analyses and water determinations, with no direct determination of the oxidation state of manganese (or iron) completed. This structural study indicates that all of the manganese is present in the divalent state, and gives eight hydrogen atoms per formula unit. The idealized formula of akatoreite is revised to $Mn_9Al_2Si_8O_{24}(OH)_8$.

Distortion of the (MnO_4) tetrahedron

The (MnO_4) tetrahedron shows significant distortions in bond length from the mean value of 2.057 Å; these can be rationalized as occurring to satisfy the bond-valence requirements of its constituent anions (Table 5). However, the O–Mn–O angles show extreme distortions (up to 36°) from the mean value of 110°. The reason for this can be seen in Figure 6. The $[Mn_2O_6]$ dimer of edge-sharing tetrahedra has to link laterally to alternate tetrahedra of the $[Si_4\phi_{13}]$ sorosilicate group, and this requires that the dimensions of the two groups match. The separation of the relevant vertices of the silicate tetrahedra is ~5.3 Å, whereas the separation of the relevant vertices of a holosymmetric $[Mn_2O_6]$ dimer is ~4.8 Å. An unconstrained sorosilicate fragment could easily shorten by differential rotation of the tetrahedra, but this is prevented in akatoreite by the articulation of the $[Si_4\phi_{13}]$ group to the strip of octahedra. On the other hand, the $[Mn_2O_6]$ dimer has no such external constraint, and hence all of the mismatch (~0.5 Å) is taken up by distortion of the edge-sharing dimer. Hence the dimer is stretched along its long axis to promote this linkage.

The $[Mn_2O_6]$ dimer also shares edges with ($Mn\phi_6$) octahedra of adjacent octahedral strips. The strong

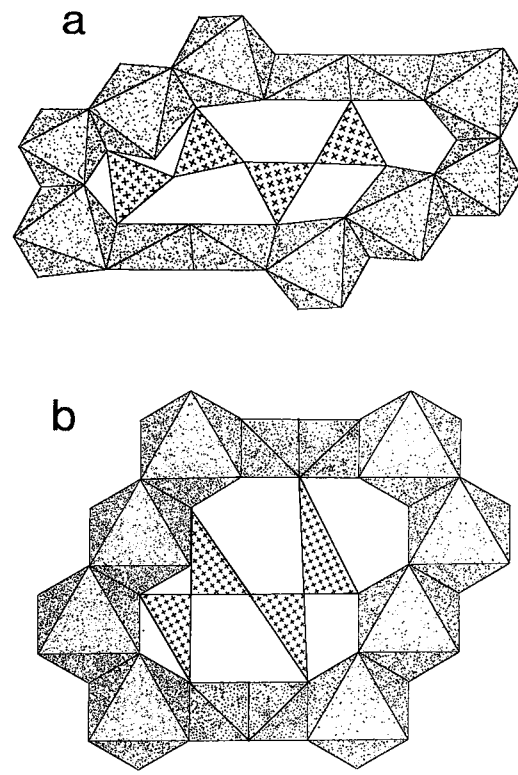

FIG. 6. Details of the articulation between the $[Si_4\phi_{13}]$ fragment and the $[Mn_2O_6]$ cluster in akatoreite projected on to (021); legend as in Figure 4. (a) Actual arrangement; (b) similar linkage with holosymmetrical octahedra.

extension of the dimer significantly decreases the potentially destabilizing Mn–Mn interactions across all of these shared edges, and it seems probable that the stabilization of this unusual arrangement of edge-sharing octahedra and tetrahedra of a large cation ($^{[4]}Mn^{2+}$ = 0.66 Å, $^{[6]}Mn^{2+}$ = 0.83 Å) results from the cooperative interaction of linkage and energetic effects.

Related sorosilicates

The detailed stereochemistry of extended $[T_n\phi_{3n+1}]$, $n > 2$ sorosilicate clusters was considered by Hawthorne (1984); details concerning bond lengths and bond angles for this structure are in agreement with the trends exhibited by the structures examined in that study. Although not noted in that previous study, all sorosilicate clusters with $n > 3$ have acid tetrahedral groups. Akatoreite is no exception; one end of the extended $[T_4\phi_{13}]$ cluster is terminated by an acid silicate group.

Sorosilicate structures with short clusters ($[Si_2\phi_7]$, $[Si_3\phi_{10}]$) are based on sheets or walls of polyhedra (octahedra or octahedra and tetrahedra) that are cross-linked by sorosilicate clusters that extend perpendicular to the sheets. Sorosilicate structures with longer clusters ($[T_6\phi_{19}]$ in medaite, $Mn_6[VSi_5O_{18}(OH)]$, Gramaccioli *et al.* 1981) consist of sheets or ribbons of octahedra in which the sorosilicate cluster extends parallel to the sheets or ribbons. In ruizite ($Ca_2Mn_2[Si_4O_{11}(OH)_2](OH)_2(H_2O)_2$: Hawthorne 1984), discontinuous sheets of edge-sharing octahedra are linked by $[Si_4\phi_{13}]$ clusters orthogonal to the sheets. On the other hand, in tiragalloite $[Mn_4AsSi_3O_{12}(OH)$: Gramaccioli *et al.* 1979] and akatoreite, the sorosilicate clusters are oriented parallel to the sheets of octahedra, and show more structural affinity with the inosilicate structures, in which infinite ($T\phi_3$) chains generally extend parallel to sheets of edge-sharing octahedra. Thus the sorosilicate composition $[T_4\phi_{13}]$ seems to be a transitional point between these two structural themes.

ACKNOWLEDGEMENTS

Financial support for this work was provided by the Natural Sciences and Engineering Research Council of Canada in the form of a Post-Graduate Fellowship to PCB and Operating, Major Equipment and Infrastructure Grants to FCH. The University of Manitoba supported this work in the form of a Post-Graduate Fellowship and the J.L. Lightcap award to PCB. Reviews by Drs. Paul B. Moore and Carlo M. Gramaccioli, and editorial work by Drs. Ronald C. Peterson and Robert F. Martin, improved the clarity and quality of the manuscript.

REFERENCES

BROWN, I.D. (1981): The bond-valence method: an empirical approach to chemical structure and bonding. *In* Structure and Bonding in Crystals II (M. O'Keeffe & A. Natvrotsky, eds.), Academic Press, New York.

CROMER, D.T. & LIBERMAN, D. (1970): Relativistic calculation of anomalous scattering factors for X rays. *J. Chem. Phys.* **53**, 1891-1898.

_____ & MANN, J.B. (1968): X-ray scattering factors computed from numerical Hartree–Fock wave functions. *Acta Crystallogr.* **A24**, 321-324.

GRAMACCIOLI, C.M., LIBORIO, G. & PILATI, T. (1981): Structure of medaite, $Mn_6[VSi_5O_{18}(OH)]$: the presence of a new kind of heteropolysilicate anion. *Acta Crystallogr.* **B37**, 1972-1978.

_____, PILATI, T. & LIBORIO, G. (1979): Structure of a manganese (II) arsenatotrisilicate, $Mn_4[AsSi_3O_{12}(OH)]$: the presence of a new tetrapolyphosphate-like anion. *Acta Crystallogr.* **B35**, 2287-2291.

HAWTHORNE, F. C. (1984): The crystal structure of ruizite, a sorosilicate with an $[Si_4\phi_{13}]$ cluster. *Tschermaks Mineral. Petrogr. Mitt.* **33**, 135-146.

SHANNON, R.D. (1976): Revised effective ionic radii and systematic studies of interatomic distances in halides and chalcogenides. *Acta Crystallogr.* **A32**, 751-767.

READ, P.B. & REAY, A. (1971): Akatoreite, a new manganese silicate from eastern Otago, New Zealand. *Am. Mineral.* **56**, 416-426.

Received June 2, 1992, revised manuscript accepted October 30, 1992.